Performance Analysis of SWIPT Relay Networks over Arbitrary Dependent Fading Channels

Farshad Rostami Ghadi and F. Javier López-Martínez

***Abstract*—In this paper, we investigate the impact of fading channel correlation on the performance of dual-hop decode-and-forward (DF) simultaneous wireless information and power transfer (SWIPT) relay networks. More specifically, by considering the power splitting-based relaying (PSR) protocol for the energy harvesting (EH) process, we quantify the effect of positive and negative dependency between the source-to-relay (SR) and relay-to-destination (RD) links on key performance metrics such as ergodic capacity and outage probability. To this end, we first represent general formulations for the cumulative distribution function (CDF) of the product of two arbitrary random variables, exploiting copula theory. This is used to derive the closed-form expressions of the ergodic capacity and outage probability in a SWIPT relay network under correlated Nakagami-m fading channels. Monte-Carlo simulation results are provided to validate the correctness of the developed analytical results, showing that the system performance significantly improves under positive dependence in the SR-RD links, compared to the case of negative dependence and independent links. Results further demonstrate that the efficiency of the ergodic capacity and outage probability ameliorates as the fading severity reduces for the PSR protocol.**

***Index Terms*—Relay network, SWIPT, ergodic capacity, outage probability, Nakagami-m model, energy harvesting, fading correlation, copula theory**

I. Introduction

Nowadays, the energy supply for electronic devices has become one of the most important challenges in designing future wireless communication systems, i.e., sixth-generation (6G) network [1]. For instance, in emerging technologies such as the Internet of Things (IoT) and its corresponding wireless applications like body wearables, peer-to-peer (P2P), device-to-device (D2D), and vehicle-to-vehicle (V2V) communications, the device nodes are mostly battery-dependent and power-constrained, and thus, they require intermittent battery replacement and recharging to maintain network connectivity, which is too expensive or even impossible in some cases. In this regard, energy harvesting (EH) from ambient energy sources has appeared as a promising approach to prolong the lifetime of energy-constrained wireless communication systems [2]–[4], equipped with replacing or recharging batteries. In contrast to traditional EH technologies that mostly relied on natural energy sources and had limited ranges of applications due to environment uncertainty, recent EH technologies exploit radio frequency (RF) signals that provide reliable energy flows and guarantee the system performance. Indeed, since the RF signals are able to carry both energy and information, simultaneous wireless information and power transfer (SWIPT) has become an alternative approach to power the next generation of wireless networks. The main idea of SWIPT was first introduced in [5] from an information-theoretic viewpoint, where the authors proposed that nodes harvest energy from their received RF information-bearing signals. However, it is not feasible for receivers' architecture to decode signals and harvest energy at the same time due to practical limitations [6]. Later, in order to address this issue, the authors in [7] proposed two practical receiver architectures with separated information decoding and energy harvesting receiver for SWIPT, namely the power splitting (PS) and the time switching (TS) architectures. In the TS protocol, the receiver switches over time between EH and information processing, whereas in the PS scheme the receiver uses a portion of the received power for EH and the remaining for information processing.

A. Related Works

In recent years, intense research activities have been carried out related to investigate the role of SWIPT in various wireless communication systems, especially cooperative relaying networks [8]–[22]. In [8], the authors considered an amplify-and-forward (AF) relay network with Rayleigh fading channels and analyzed the key performance metrics such as ergodic capacity and outage probability under both PS and TS protocols to determine the proposed system throughput, where it was showed that the SWIPT-based relaying provides throughput improvement, communication reliability enhancement, and coverage range extension. In contrast, the authors in [9] derived the closed-form expression of the outage probability over independent Rayleigh SWIPT-relaying networks, where both AF and decode-and-forward (DF) protocols were considered. A more general SWIPT-relaying network, i.e., multiuser multirelay cooperative network, over Rayleigh fading channels was considered in [10], where the authors investigated the outage probability performance under DF, variable-gain AF, and fixed-gain AF protocols. Proposing two information receiving strategies, i.e., the mutual information accumulation (IA) and the energy accumulation (EA), the

Manuscript received June xx, 2022; revised XXX.

This work was funded in part by Junta de Andalucía, the European Union and the European Fund for Regional Development FEDER through grants EMERGIA20-00297 and P18-RT-3175, and in part by MCIN/AEI/10.13039/501100011033 through grant PID2020-118139RB-I00.

Farshad Rostami Ghadi is with the Department of Electronic and Electrical Engineering, University College London, WC1E 6BT London, UK. (E-mail: f.rostamighadi@ucl.ac.uk).

F.J. López-Martínez is with the Dept. Signal Theory, Networking and Communications, Research Centre for Information and Communication Technologies (CITIC-UGR), University of Granada, 18071, Granada (Spain), and also with the Communications and Signal Processing Lab, Telecommunication Research Institute (TELMA), Universidad de Málaga, Málaga, 29010, (Spain). (E-mail: fjlm@ugr.es).

Corresponding author: Farshad Rostami Ghadi

Digital Object Identifier 10.1109/XXX.2021.XXXXXXX

authors in [11] evaluated the achievable rate region of the SWIPT relaying network under Rayleigh fading channels. Considering log-normal fading channels in a dual-hop SWIPT relaying network, the ergodic outage probability performance for both full-duplex (FD) and half-duplex (HD) relaying mechanisms with DF and AF relaying protocols under PS and TS schemes was investigated in [12]. The outage probability performance for SWIPT relaying networks in the presence of direct link between the source and the destination under Rayleigh fading channels was analyzed in [13] and [14]. Furthermore, assuming the direct link between the source and the destination, the performance of SWIPT relaying networks in terms of the outage probability and bit error rate under Nakagami-m fading channels was investigated in [15] and [16], respectively. On the other hand, key performance metrics for SWIPT relaying networks under generalized κ-μ, α-μ, and Fisher-Snedecor $\mathcal{F}$ composite fading channels were analyzed in [17], [18], and [19], respectively. Finally, the performance of SWIPT-based schemes in two-way relaying was investigated in [20]–[22] in several practical scenarios.

B. Motivation

Recent research has shown that the performance of SWIPT-based relaying networks highly depends on the statistical characteristics of channels in radio propagation environments. Therefore, accurate modeling of fading channels in SWIPT-based relaying networks is a momentous issue that should be considered. However, in all the above-mentioned literature related to the performance analysis of SWIPT relaying networks, it was ignored the potential dependence structure of the source-to-relay (SR) hop on the relay-to-destination (RD) hop, while the channel coefficients observed by the relay and the destination may be correlated in practice [23], [24]. In addition, from a communication-theoretic perspective, the equivalent channel observed by the destination over a SWIPT-relaying network is the product of two correlated random variables (RVs), which largely complicates the performance evaluation of such a system. Although great efforts have been carried out to find the distribution of the product of two correlated RVs, most previous contributions only derived the corresponding CDF under specific distributions or obtained approximation forms for that due to mathematical and statistical limitations [25]–[27]. Therefore, being able to generate such a CDF that can be valid for any arbitrary random variable is extremely challenging. On the other hand, the underlying dependence between fading channel coefficients may not be linear, and thus, the classic Pearson correlation coefficient fails to appropriately model the interdependence of fading events caused by different mechanisms, especially as to the tails of the fading distributions [28]. Hence, the role of general dependence structures beyond linear correlation is gaining momentum in the wireless community. In this regard, one flexible method for incorporating both positive/negative dependence structures between RVs, generating the distribution of the product of two correlated RVs with arbitrary distribution, and describing the non-linear dependency between arbitrary RVs is copula theory, which has been recently used in the performance analysis of wireless communication systems [29]–[37]. Copula functions are mostly defined with a specific dependence parameter which indicates the measure of dependency between correlated RVs. In this regard, the main advantages of using copula theory rather than traditional statistical methods are: (i) Providing a more general case by describing both linear and non-linear structure of dependence between two or more arbitrary RVs; (ii) Generating the multivariate distributions of two or more arbitrary random variables by only knowing the marginal distributions; (iii) Describing both positive and negative dependencies between two or more arbitrary RVs. Exploiting such benefits, the authors in [29] analyzed the capacity of correlated Nakagami-m fading MIMO channels by using specific copula functions under linear and positive dependence structures. The outage probability and coverage region for correlated Rayleigh fading multiple access channels were also derived in [30] by using the Farlie-Gumbel-Morgenstern (FGM) copula function. The authors in [31] also applied the FGM copula to secure communications and derived closed-form expressions for the secrecy outage probability and average secrecy capacity under correlated Rayleigh fading channels. In [32] and [33], the authors provided the upper and lower bounds of the outage probability for the multiple access communications under correlated Rayleigh fading distributions. Using the FGM copula function, the authors in [34] analyzed the outage probability and coverage region of multiple access communications in the presence of the non-causally known side information at the transmitters. The upper and lower bounds for secrecy performance metrics were also derived in [35] by using the Fréchet-Hoeffding (FH) bounds. In [36], the authors obtained a general formulation for the product fading channels for backscatter communication systems and derived the closed-form expression of the average capacity using the FGM copula. In addition, by exploiting Clayton copula, the outage probability and average capacity for different multiple access communications under correlated Fisher-Snedecor $\mathcal{F}$ fading channels were analyzed in [37]. Even so, most previous works in this context only considered a specific copula function [29]–[31], [34], [37] or considered FH bounds to analyze their proposed system models [32], [33], [35], but fail to analyze the system performance under arbitrary fading correlation. References dedicated to investigate the role of correlation in the context of wireless powered communications are scarce, and mostly restricted to point-to-point links with linear dependence [38], or based on simulations [39]. However, depending on the specific set-up, correlation between links in relay-based scenarios is experimentally shown to appear in backscatter communications due to pinhole effect [40], [41], or due to the slow variability of fading in SWIPT scenarios with bidirectional operation between the energy source and the energy-constrained device [38], [42]. With all the aforementioned considerations, there are several unanswered practical questions over SWIPT-based relaying networks to date: (i) What is the effect of fading correlation on the key performance metrics of SWIPT in cooperative relaying communications? (ii) How does fading severity affect the performance of SWIPT relaying communications under such correlation? To the best of the authors' knowledge, there

has been no previous research in analyzing SWIPT-relaying networks with arbitrarily distributed and correlated fading channels.

C. Contribution

Motivated by the aforesaid observations, the key contribution of this work is to show how dependence structures between fading links impact the performance of SWIPT relay networks under *any arbitrarily-distributed correlated fading channels*. To this end, we consider the scenario that the energy-constrained relay node harvests energy from the RF signal broadcasted by a source node and uses that harvested energy to forward the source signal to a destination node, where the SR and RD links are correlated RVs with arbitrary distributions. Based on the DF relaying protocol, we adopt the PS-based relaying (PSR) scheme, as proposed in [8], for separate information processing and energy harvesting at the energy-constrained relay node. Using a mathematical approach based on that adopted in [36], we introduce a general formulation for the cumulative distribution function (CDF) of the product of two correlated RVs with any arbitrary distribution, exploiting the copula theory. Then, in order to analyze the system performance, we derive the closed-form expression of the ergodic capacity and outage probability under Nakagami-m fading channels, using a specific copula function. Specifically, the contributions of our work are summarized as follows:

- We provide general formulations for the CDF of the equivalent channel observed by the destination (i.e, the product of two arbitrarily distributed and correlated RVs).
- In order to realize the impact of the fading correlation on the system performance, we derive the closed-form expressions of the ergodic capacity and outage probability assuming the PSR protocol under correlated Nakagami-m fading, exploiting the Farlie-Gumbel-Morgenstern (FGM) copula.
- By changing the dependence parameter within the defined range, our numerical and simulation results show that the system performance improves in terms of the ergodic capacity and the outage probability under the positive dependence structure, while the negative correlation has destructive effects on the system efficiency. In addition, a reduction in fading severity improves the system performance under the PSR scheme.

D. Paper Organization

The rest of this paper is organized as follows. Section II describes the system model considered in our work. In section III, the main concept of copula theory is reviewed, and then the signal-to-noise ratio (SNR) distribution is derived. Section IV presents the main results of the considered SWIPT-based relaying network under correlated Nakagami-m fading channels so that the closed-form expressions of the ergodic capacity and outage probability are determined in subsections IV-A and IV-B, respectively. In section V, the efficiency of analytical results is illustrated numerically, and finally, the conclusions are drawn in section VI.

II. System Model

A. Channel Model

We consider a relay network as shown in Fig. 1(a), where a source node S wants to send information to a destination node D through an intermediate relay node R. It is assumed that there is no direct link between the source S and the destination D due to deep shadow fading or surrounding physical obstacles. Such an assumption is widely adopted in research studies related to SWIPT relay communications [8], [12], [43]. Specifically, this presumption is related to the coverage extension models where there is a long distance between the source and destination, and relays are exploited in order to maintain connectivity. This model is used in Internet-of-Thing (IoT) deployments, where RF-powered relays are employed to provide coverage expansion to avoid interference. As will become evident in the sequel, because of the time-division fashion on which the half-duplex relay protocol is implemented, interference is avoided at the information receiver. For simplicity purposes, we assume that all nodes are equipped with single antennas. We also suppose that the nodes S and D have sufficient energy supply from other sources (e.g., a battery or a power grid), while the relay R has no external power supply and only relies on the harvested signal transmitted by source S, thus relay R is energy-constrained. The transmission consists of two phases and the HD deployment based on the DF strategy is adopted for the relay node R. The channel coefficients of SR and RD are defined by $h_{\rm SR}$ and $h_{\rm RD}$, respectively, and they are considered arbitrarily distributed and correlated RVs. Besides, we assume all channels are quasi-static fading channels, that is, the fading coefficients are fixed during the transmission of an entire codeword (i.e., $h_{\rm SR}(i) = h_{\rm SR}$ and $h_{\rm RD}(i) = h_{\rm RD}$, $\forall i = 1, ..., n$), and vary randomly from one block to another block.

B. Information and Energy Transfer

We exploit the PSR protocol for transferring information and energy in the considered model. In this protocol, the total communication process time T is split into two consecutive time slots. Let $0 < \rho \leq 1$ and $P_{\rm S}$ denote the power-splitting factor and source power, respectively. In the first slot, the relay node R uses a portion of the source power $(1-\rho)P_{\rm S}$ for information processing (i.e., decoding), and the remaining source power $\rho P_{\rm S}$ is harvested, so it can be used in the second time slot for relaying the decoded information. (see Figs. 1(b) and 1(c)). Thus, the instantaneous SNR at the relay R and the destination D can be defined as

$$\gamma_{\rm R} = \frac{(1-\rho)P_{\rm S}|h_{\rm SR}|^2}{d_{\rm SR}^{\alpha}N} = \hat{\gamma}_{\rm R} g_{\rm SR}, \tag{1}$$

$$\gamma_{\rm D} = \frac{\kappa\rho P_{\rm S}|h_{\rm SR}|^2|h_{\rm RD}|^2}{d_{\rm SR}^{\alpha}d_{\rm RD}^{\alpha}N} = \hat{\gamma}_{\rm D} g_{\rm SR} g_{\rm RD}, \tag{2}$$

where $d_{\rm SR}$ and $d_{\rm RD}$ are the distances of SR and RD, respectively, and α is the path-loss exponent. The terms $g_{\rm SR} = |h_{\rm SR}|^2$ and $g_{\rm RD} = |h_{\rm RD}|^2$ define the normalized fading power channel coefficients associated to the SR and RD

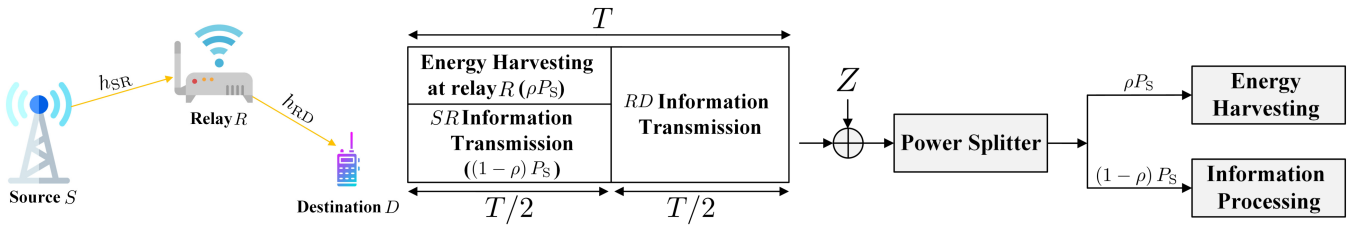

Fig. 1. (a) Illustration of a SWIPT-based relaying network. (b) Illustration of the PSR protocol for energy harvesting and information processing at the relay R. (c) Block diagram of the relay R under the PSR protocol, where Z denotes noise with power N.

links, respectively. Besides, $0 < \kappa \leq 1$ is the EH efficiency[1] and N denotes the noise power. The average SNR at the destination is given by $\mathbb{E}\{\gamma_{\rm D}\} = \hat{\gamma}_{\rm D}\mathbb{E}\{g_{\rm SR}g_{\rm RD}\}$. Note that $\mathbb{E}\{g_{\rm SR}g_{\rm RD}\} = 1$ only in the case of independence; however, in the cases with positive/negative dependence, this factor will depend on the actual relation between $g_{\rm SR}$ and $g_{\rm RD}$. For the sake of generality, the statistical dependence between the SR and RD links is agnostic to the source of dependence. This can be due to channel reciprocity as in [38], [39], or specific propagation conditions [45], [46].

III. SNR DISTRIBUTION

In this section, we derive general analytical expressions for the CDF of SNR $\gamma_{\rm D}$ by exploiting the copula theory.

A. Copula definition and properties

In order to determine the distribution of $\gamma_{\rm D}$ in the general case, we first briefly review some fundamental definitions and properties of the two-dimensional copulas [47].

Definition 1 (Two-dimensional copula)**.** *The copula function $C(u_1, u_2)$ of a random vector $\mathbf{X}\,(X_1, X_2)$ defined on the unit hypercube $[0,1]^2$ with uniformly distributed RVs $U_j := F_{X_j}(x_j)$ for $j \in \{1,2\}$ over $[0,1]$ is given by*

$$C(u_1, u_2) = \Pr(U_1 \leq u_1, U_2 \leq u_2). \tag{3}$$

where $F_{X_j}(x_j) = \Pr(X_j \leq x_j)$ denotes the marginal CDF.

Theorem 1 (Sklar's theorem)**.** *Let $F_{X_1,X_2}(x_1, x_2)$ be a joint CDF of RVs with marginals $F_{X_j}(x_j)$ for $j \in \{1,2\}$. Then, there exists one copula function $C(\cdot,\cdot)$ such that for all x_j in the extended real line domain $\mathbb{R}$,*

$$F_{X_1,X_2}(x_1, x_2) = C\left(F_{X_1}(x_1), F_{X_2}(x_2)\right). \tag{4}$$

Definition 2 (Survival copula)**.** *Let $\mathbf{X} = (X_1, X_2)$ be a vector of two absolutely continuous RVs with joint CDF $F_{X_1,X_2}(x_1, x_2)$ and marginal survival functions $\overline{F}_{X_j}(x_j) = \Pr(X_j > x_j) = 1 - F_{X_j}(x_j)$ for $j = 1, 2$, the joint survival function $\overline{F}_{X_1,X_2}(x_1, x_2)$ is given by*

$$\overline{F}_{X_1,X_2}(x_1, x_2) = \Pr(X_1 > x_1, X_2 > x_2) \tag{5}$$

$$= \hat{C}(\overline{F}_{X_1}(x_1), \overline{F}_{X_2}(x_2)), \tag{6}$$

where $\hat{C}(u_1, u_2) = u_1 + u_2 - 1 + C(1-u_1, 1-u_2)$ is the survival copula of $\mathbf{X}$.

Definition 3 (Dependence structures)**.** *Consider two copula functions that verify*

$$C_1 \prec C^{\perp} \prec C_2, \tag{7}$$

where $C^{\perp}(u_1, u_2) = u_1 \cdot u_2$ is the product copula and describes the independent structure. Then, C_1 and C_2 model the negative and positive dependence structures, respectively.

B. Arbitrary dependence

Since the considered fading channels are correlated, the distribution of the SNR at the destination D is that of the product of two arbitrary correlated RVs. For this purpose, we exploit the following theorems to determine the CDF of the SNR $\gamma_{\rm D}$.

Theorem 2. *Let $\mathbf{X} = (X_1, X_2)$ be a vector of two absolutely continuous RVs with the corresponding copula C and CDFs $F_{X_j}(x_j)$ for $j \in \{1,2\}$. Thus, the CDF of $Y = X_1X_2$ is*

$$F_Y(y) = F_{X_1}(0) + \int_0^1 \operatorname{sgn}\left(F_{X_1}^{-1}(u)\right) \frac{\partial}{\partial u} C\left(u, F_{X_2}\left(\frac{y}{F_{X_1}^{-1}(u)}\right)\right) du, \tag{8}$$

where $F_{X_1}^{-1}(.)$ is an inverse function of $F_{X_1}(.)$ and $\operatorname{sgn}(.)$ defines the Sign function.

Proof. The details of proof are in Appendix A. □

Corollary 1. *The CDF of $\gamma_{\rm D}$ in the general dependence case of fading channels is given by*

$$F_{\gamma_{\rm D}}(\gamma_{\rm D}) = F_{G_{\rm SR}}(0) + \int_0^1 \operatorname{sgn}\left(g_{\rm SR}\right) f_{G_{\rm SR}}(g_{\rm SR}) \times \frac{\partial}{\partial F_{G_{\rm SR}}(g_{\rm SR})} C\left(F_{G_{\rm SR}}(g_{\rm SR}), F_{G_{\rm RD}}\left(\frac{\gamma_{\rm D}}{\hat{\gamma}_{\rm D} g_{\rm SR}}\right)\right) dg_{\rm SR}. \tag{9}$$

Proof. Let $Y = G_{\rm SR}G_{\rm RD}$ and $u = F_{G_{\rm SR}}(g_{\rm SR})$ in Theorem 2, and using the fact that $F_{\gamma_{\rm D}}(\gamma_{\rm D}) = F_Y\left(\frac{\gamma_{\rm D}}{\hat{\gamma}_{\rm D}}\right)$, the proof is completed. □

Note that Corollary 1 is valid for any arbitrary choice of fading distributions as well as copula functions. However, for

[1]Recent results in [44] show that transmitter high-power amplifier's (HPA) non-linearities become dominant over EH's non-linearities when low-PAPR waveforms are use. Hence, the linear approximation for the EH behavior is reasonably good in practice and also serves as an upper bound of performance for the case of non-linear EH.

$$F_{\gamma_{\rm D}}(\gamma_{\rm D}) = 1 - \sqrt{2\mathcal{B}}\Bigg(\sum_{n=0}^{m-1} a_n {\gamma_{\rm D}}^{\frac{m+n}{2}} K_{n-m}\left(\zeta\sqrt{\gamma_{\rm D}}\right) + \theta\Bigg[\sum_{n=0}^{m-1} a_n {\gamma_{\rm D}}^{\frac{m+n}{2}} K_{n-m}\left(\zeta\sqrt{\gamma_{\rm D}}\right) - \sum_{k=0}^{m-1}\sum_{n=0}^{m-1} b_{k,n} {\gamma_{\rm D}}^{\frac{k+n+m}{2}} K_{n-k-m}\left(\zeta\sqrt{2\gamma_{\rm D}}\right) - \sum_{n=0}^{m-1}\sum_{l=0}^{m-1} c_{n,l} {\gamma_{\rm D}}^{\frac{l+m+n}{2}} K_{l-m+n}\left(\zeta\sqrt{2\gamma_{\rm D}}\right) + \sum_{k=0}^{m-1}\sum_{n=0}^{m-1}\sum_{l=0}^{m-1} d_{k,n,l} {\gamma_{\rm D}}^{\frac{k+n+l+m}{2}} K_{n+l-k-m}\left(2\zeta\sqrt{\gamma_{\rm D}}\right) \Bigg]\Bigg). \tag{14}$$

exemplary purposes, we assume in the sequel that the SR and RD fading channel coefficients (i.e., $h_{\rm SR}$ and $h_{\rm RD}$) follow the Nakagami-m distribution, where the parameter $m \geq 0.5$ denotes fading severity. Note that any choice of generalized fading distribution can be used, by following the same steps as described for the Nakagami-m case, although at the expense of increased mathematical complexity. Hence, the corresponding fading power channel coefficients g_i for $i \in \{SR, RD\}$ are dependent Gamma RVs, and we have following marginal distributions

$$f_{G_i}(g_i) = \frac{{m_i}^{m_i}}{\Gamma(m_i)\overline{g}_i{}^{m_i}} {g_i}^{m_i-1} e^{-\frac{m_i}{\overline{g}_i}g_i}, \tag{10}$$

$$F_{G_i}(g_i) = 1 - \frac{\Gamma(m_i, \frac{m_i}{\overline{g}_i}g_i)}{\Gamma(m_i)} \tag{11}$$

$$= 1 - e^{-\frac{m_i}{\overline{g}_i}g_i} \sum_{k=0}^{m_i-1} \frac{1}{k!}\left(\frac{m_i}{\overline{g}_i}g_i\right)^k, \tag{12}$$

where $\overline{g}_i = \mathbb{E}[g_i]$ are the average of corresponding fading power channel coefficients, and m_i are shape parameters. Note that (12) is only valid for integer values of m, while (11) is valid for any arbitrary m. In the sequel, (12) will be preferred for the sake of simplicity, although similar steps can be carried out using a series expansion for the Gamma function in (11) if desired.

Although there are many copula functions that can be used to evaluate the structure of dependency beyond linear correlation, we exploit the FGM copula in our analysis. This choice is justified because it allows capturing both negative and positive dependencies between the RVs while offering good mathematical tractability, at the expense of a certain inability to model scenarios with strong dependencies [48]. In any case, the choice of Copula is known to depend on the specific geometry and propagation conditions for the scenario under consideration, although the ability to capture *both* positive and negative dependence structures is required [32]. As will be shown in section V, the use of the FGM copula is enough for our purposes of determining the effect of negative/positive correlation between SR and RD links.

Definition 4. *[FGM copula] The bivariate FGM copula with dependence parameter $\theta \in [-1, 1]$ is defined as*

$$C_{\mathcal{F}}(u_1, u_2) = u_1 u_2 (1 + \theta(1 - u_1)(1 - u_2)), \tag{13}$$

where $\theta \in [-1, 0)$ and $\theta \in (0, 1]$ denote the negative and positive dependence structures respectively, while $\theta = 0$ always indicates the independence structure.

Theorem 3. *The CDF of $\gamma_{\rm D}$ under correlated Nakagami-m fading channels using the FGM copula is given by* (14)*, where $\mathcal{B} = \frac{2m^{2m}}{\hat{\gamma}_{\rm D}^m \Gamma(m)^2}$, $\zeta = \frac{2m}{\sqrt{\hat{\gamma}_{\rm D}}}$, and $K_v(.)$ is the modified Bessel function of the second kind and order v. The coefficients a_n, $b_{k,n}$, $c_{n,l}$, and $d_{k,n,l}$ are also respectively defined as*

$$a_n = \frac{m^n}{\hat{\gamma}_{\rm D}^{\frac{n}{2}} n!}, \quad b_{k,n} = \frac{m^{k+n} 2^{\frac{n-k-m+2}{2}}}{\hat{\gamma}_{\rm D}^{\frac{k+n}{2}} k! n!},$$
$$c_{n,l} = \frac{m^{l+n} 2^{\frac{-l+m-n}{2}}}{\hat{\gamma}_{\rm D}^{\frac{n+l}{2}} n! l!}, \quad d_{k,n,l} = \frac{2m^{k+n+l}}{\hat{\gamma}_{\rm D}^{\frac{k+n+l}{2}} k! n! l!}.$$

Proof. The details of proof are in Appendix B. □

The probability density function (PDF) of $\gamma_{\rm D}$ was also obtained in [36, Thm. 4] as (15), where the coefficients q_k and $t_{k,n}$ are given by $q_k = \frac{2^{2-\frac{k}{2}} m^k}{\hat{\gamma}_{\rm D}^{\frac{k}{2}} k!}$ and $t_{k,n} = \frac{4m^{k+n}}{\hat{\gamma}_{\rm D}^{\frac{k+n}{2}} k! n!}$, respectively. It should be noted that the closed-form expressions of the CDF and PDF provided in (14) and (15) are valid for integer values of m, while the integral-form expressions can be used for arbitrary positive real values of m. In addition, the PDF and the CDF of $\gamma_{\rm R}$ are also given by

$$f_{\gamma_{\rm R}}(\gamma_{\rm R}) = \frac{m^m}{\Gamma(m)\hat{\gamma}_{\rm R}^m} {\gamma_{\rm R}}^{m-1} {\rm e}^{-\frac{m}{\hat{\gamma}_{\rm R}}\gamma_{\rm R}}, \tag{16}$$

$$F_{\gamma_{\rm R}}(\gamma_{\rm R}) = 1 - {\rm e}^{-\frac{m}{\hat{\gamma}_{\rm R}}\gamma_{\rm R}} \sum_{k=0}^{m-1} \frac{1}{k!}\left(\frac{m}{\hat{\gamma}_{\rm R}}\gamma_{\rm R}\right)^k. \tag{17}$$

Corollary 2. *The average SNR $\overline{\gamma}_{\rm D} = \hat{\gamma}_{\rm D}\mathbb{E}\{g_{\rm SR} g_{\rm RD}\}$ is given by*

$$\overline{\gamma}_{\rm D} = \hat{\gamma}_{\rm D}\left(1 + \theta\left(1 - \mho(m)\right)\right), \tag{18}$$

where

$$\mho(m) = \sum_{k=0}^{m-1} \frac{2^{-(m+k-1)}}{m{\rm B}(m,k+1)} - \sum_{k=0}^{m-1}\sum_{n=0}^{m-1} \frac{2^{-(2m+k+n)}}{m^2{\rm B}(m,k+1){\rm B}(m,n+1)}, \tag{19}$$

and ${\rm B}(\cdot,\cdot)$ is the Beta function.

Proof. Using (15) and the definition of expectation, and after some manipulations, (18) is obtained. □

Corollary 2 shows that the average SNR at the destination is increased (decreased) due to positive (negative) dependence by a scaling factor that depends on the fading severity, compared to the case of independence. This indicates that the role of positive/negative dependence has an impact on the average SNR, which in turn will impact the system performance, as discussed next. In the sequel, we exemplify how the key performance metrics of interest, i.e., the ergodic capacity and outage probability, can be characterized in the closed-form expressions for the specific case of using the Nakagami-m fading and the FGM copula.

$$f_{\gamma_{\rm D}}(\gamma_{\rm D}) = \mathcal{B}\Bigg(\gamma_{\rm D}^{m-1}K_0\left(\zeta\sqrt{\gamma_{\rm D}}\right) + \theta\Bigg[\gamma_{\rm D}^{m-1}K_0\left(\zeta\sqrt{\gamma_{\rm D}}\right) - \sum_{k=0}^{m-1} q_k \gamma_{\rm D}^{\frac{k}{2}+m-1} K_k\left(\zeta\sqrt{2\gamma_{\rm D}}\right) + \sum_{k=0}^{m-1}\sum_{n=0}^{m-1} t_{k,n}\gamma_{\rm D}^{\frac{k+n}{2}+m-1} K_{n-k}\left(2\zeta\sqrt{\gamma_{\rm D}}\right)\Bigg]\Bigg). \tag{15}$$

IV. Performance Analysis: Ergodic Capacity and Outage Probability

In this section, we derive analytical expressions for the ergodic capacity and the outage probability for the considered system model under dependent Nakagami-m fading channels.

A. Ergodic Capacity

In the considered dual-hop relay network, the instantaneous capacity is defined as [49]

$$\mathcal{C} = \min(\mathcal{C}_{\rm SR}, \mathcal{C}_{\rm RD}), \tag{20}$$

where $\mathcal{C}_{\rm SR}$ and $\mathcal{C}_{\rm RD}$ are the instantaneous capacity of the SR and RD links, respectively, which can defined as follows

$$\mathcal{C}_{\rm SR} = \frac{1}{2}\log_2\left(1+\gamma_{\rm R}\right), \tag{21}$$

$$\mathcal{C}_{\rm RD} = \frac{1}{2}\log_2\left(1+\gamma_{\rm D}\right). \tag{22}$$

Theorem 4. *The ergodic capacity of the SR link for the considered system model under Nakagami-m fading channel is given by*

$$\overline{\mathcal{C}}_{\rm SR} = \frac{1}{2\Gamma(m)\ln 2} G_{3,2}^{1,3}\left(\begin{array}{c|c} \frac{\hat{\gamma}_{\rm R}}{m} & \left(1-\frac{m}{\hat{\gamma}_{\rm R}},1,1\right) \\ & (1,0) \end{array}\right). \tag{23}$$

Proof. The ergodic capacity given in (21) can be further mathematically expressed as

$$\overline{\mathcal{C}}_{\rm SR} = \frac{1}{2\ln 2}\int_0^\infty \ln\left(1+\gamma_{\rm R}\right) f_{\gamma_{\rm R}}(\gamma_{\rm R}) d\gamma_{\rm R}, \tag{24}$$

where $f_{\gamma_{\rm R}}(\gamma_{\rm R})$ is given by (16). Next, by re-expressing the logarithm function in terms of the Meijer's G-function [50, Eq. (11)], i.e.,

$$\ln(1+x) = G_{2,2}^{1,2}\left(\begin{array}{c|c} x & (1,1) \\ & (1,0) \end{array}\right), \tag{25}$$

substituting (16) and (25) in (24), $\overline{\mathcal{C}}_{\rm SR}$ can be re-written as

$$\overline{\mathcal{C}}_{\rm SR} = \frac{m^m}{2\hat{\gamma}_{\rm R}^m\Gamma(m)\ln 2} \times \underbrace{\int_0^\infty \gamma_{\rm R}^{m-1}\mathrm{e}^{-\frac{m}{\hat{\gamma}_{\rm R}}\gamma_{\rm R}} G_{2,2}^{1,2}\left(\begin{array}{c|c} \gamma_{\rm R} & (1,1) \\ & (1,0) \end{array}\right) d\gamma_{\rm R}}_{\mathcal{I}}. \tag{26}$$

With the help of [51, Eq. (2.24.3.1)], $\mathcal{I}$ can be computed as

$$\mathcal{I} = \frac{\hat{\gamma}_{\rm R}^m}{m^m} G_{3,2}^{1,3}\left(\begin{array}{c|c} \frac{\hat{\gamma}_{\rm R}}{m} & \left(1-\frac{m}{\hat{\gamma}_{\rm R}},1,1\right) \\ & (1,0) \end{array}\right). \tag{27}$$

Now, by inserting (27) into (26) the proof is completed. □

Theorem 5. *The ergodic capacity of the RD link for the considered system model under Nakagami-m fading channel is given by* (26)*, where $\mathcal{D}$, w_k, and $z_{k,n}$ are respectively defined as*

$$\mathcal{D} = \frac{2^{2m-2}\mathcal{B}}{\pi\zeta^{2m}\ln 2}, \quad w_k = \frac{2^{2-m}m^k}{\hat{\gamma}_{\rm D}^{\frac{k}{2}}\zeta^k k!}, \quad z_{k,n}\frac{2^{2-2m}m^{k+n}}{\hat{\gamma}_{\rm D}^{\frac{k+n}{2}}\zeta^{n+k}k!n!}.$$

Proof. The ergodic capacity given in (22) can be further mathematically defined as

$$\overline{\mathcal{C}}_{\rm RD} = \frac{1}{2\ln 2}\int_0^\infty \ln\left(1+\gamma_{\rm D}\right) f_{\gamma_{\rm D}}(\gamma_{\rm D}) d\gamma_{\rm D}, \tag{27}$$

where $f_{\gamma_{\rm D}}(\gamma_{\rm D})$ is determined by Theorem 3 as (15). Thus, by plugging (25) and (15) into (27), $\overline{\mathcal{C}}_{\rm RD}$ can be re-expressed as

$$\overline{\mathcal{C}}_{\rm RD} = \frac{\mathcal{B}}{2\ln 2}\Bigg(\mathcal{J}_1 + \theta\Bigg[\mathcal{J}_1 - \sum_{k=0}^{m-1}\frac{2^{2-\frac{k}{2}}m^k}{\hat{\gamma}_{\rm D}^{\frac{k}{2}}k!}\mathcal{J}_2 + \sum_{k=0}^{m-1}\sum_{n=0}^{m-1}\frac{4m^{k+n}}{\hat{\gamma}_{\rm D}^{\frac{k+n}{2}}k!n!}\mathcal{J}_3\Bigg]\Bigg), \tag{28}$$

in which

$$\mathcal{J}_1 = \int_0^\infty \gamma_{\rm D}^{m-1}K_0\left(\zeta\sqrt{\gamma_{\rm D}}\right) G_{2,2}^{1,2}\left(\begin{array}{c|c} \gamma_{\rm D} & (1,1) \\ & (1,0) \end{array}\right) d\gamma_{\rm D}, \tag{29}$$

$$\mathcal{J}_2 = \int_0^\infty \gamma_{\rm D}^{\frac{k}{2}+m-1}K_k\left(\zeta\sqrt{2\gamma_{\rm D}}\right) G_{2,2}^{1,2}\left(\begin{array}{c|c} \gamma_{\rm D} & (1,1) \\ & (1,0) \end{array}\right) d\gamma_{\rm D}, \tag{30}$$

and

$$\mathcal{J}_3 = \int_0^\infty \gamma_{\rm D}^{\frac{k+n}{2}+m-1} \times K_{n-k}\left(2\zeta\sqrt{\gamma_{\rm D}}\right) G_{2,2}^{1,2}\left(\begin{array}{c|c} \gamma_{\rm D} & (1,1) \\ & (1,0) \end{array}\right) d\gamma_{\rm D}. \tag{31}$$

With the help of [51, (2.24.4.3)], the integrals $\mathcal{J}_1$, $\mathcal{J}_2$, and $\mathcal{J}_3$ can be respectively computed as follows

$$\mathcal{J}_1 = \frac{2^{2m}}{2\pi\zeta^{2m}} G_{4,2}^{1,4}\left(\begin{array}{c|c} \frac{4}{\zeta^2} & (1-m,1-m,1,1) \\ & (1,0) \end{array}\right), \tag{32}$$

$$\mathcal{J}_2 = \frac{2^{m+\frac{k}{2}}}{2\pi\zeta^{2m+k}} G_{4,2}^{1,4}\left(\begin{array}{c|c} \frac{2}{\zeta^2} & (1-(m+k),1-m,1,1) \\ & (1,0) \end{array}\right), \tag{33}$$

$$\overline{\mathcal{C}}_{\mathrm{RD}} = \left(G_{4,2}^{1,4}\left(\frac{4}{\zeta^2} \;\middle|\; \begin{matrix}(1-m,1-m,1,1)\\(1,0)\end{matrix} \right) + \theta\left[G_{4,2}^{1,4}\left(\frac{4}{\zeta^2} \;\middle|\; \begin{matrix}(1-m,1-m,1,1)\\(1,0)\end{matrix} \right) - \sum_{k=0}^{m-1} w_k G_{4,2}^{1,4}\left(\frac{2}{\zeta^2} \;\middle|\; \begin{matrix}(1-(m+k),1-m,1,1)\\(1,0)\end{matrix} \right) + \sum_{k=0}^{m-1}\sum_{n=0}^{m-1} z_{k,n} G_{4,2}^{1,4}\left(\frac{1}{\zeta^2} \;\middle|\; \begin{matrix}(1-(m+n),1-(m+k),1,1)\\(1,0)\end{matrix} \right) \right] \right). \tag{26}$$

$$\begin{aligned} P_{\mathrm{o}} =& 1 - \left[\frac{\Gamma(m, \frac{m}{\hat{\gamma}_{\mathrm{R}}}\gamma_{\mathrm{t}})\sqrt{2\mathcal{B}}}{\Gamma(m)} \left(\sum_{n=0}^{m-1} a_n \gamma_{\mathrm{t}}^{\frac{m+n}{2}} K_{n-m}\left(\zeta\sqrt{\gamma_{\mathrm{t}}}\right) + \theta\left[\sum_{n=0}^{m-1} a_n \gamma_{\mathrm{t}}^{\frac{m+n}{2}} K_{n-m}\left(\zeta\sqrt{\gamma_{\mathrm{t}}}\right) \right.\right.\right. \\ & - \sum_{k=0}^{m-1}\sum_{n=0}^{m-1} b_{k,n} \gamma_{\mathrm{t}}^{\frac{k+n+m}{2}} K_{n-k-m}\left(\zeta\sqrt{2\gamma_{\mathrm{t}}}\right) - \sum_{n=0}^{m-1}\sum_{l=0}^{m-1} c_{n,l} \gamma_{\mathrm{t}}^{\frac{l+m+n}{2}} K_{l-m+n}\left(\zeta\sqrt{2\gamma_{\mathrm{t}}}\right) \\ & \left.\left.\left. + \sum_{k=0}^{m-1}\sum_{n=0}^{m-1}\sum_{l=0}^{m-1} d_{k,n,l} \gamma_{\mathrm{t}}^{\frac{k+n+l+m}{2}} K_{n+l-k-m}\left(2\zeta\sqrt{\gamma_{\mathrm{t}}}\right) \right] \right) \left(1 + \theta\left(1 - \sqrt{2\mathcal{B}}\left(\sum_{n=0}^{m-1} a_n \gamma_{\mathrm{t}}^{\frac{m+n}{2}} K_{n-m}\left(\zeta\sqrt{\gamma_{\mathrm{t}}}\right) \right.\right.\right. \right. \\ & + \theta\left[\sum_{n=0}^{m-1} a_n \gamma_{\mathrm{t}}^{\frac{m+n}{2}} K_{n-m}\left(\zeta\sqrt{\gamma_{\mathrm{t}}}\right) - \sum_{k=0}^{m-1}\sum_{n=0}^{m-1} b_{k,n} \gamma_{\mathrm{t}}^{\frac{k+n+m}{2}} K_{n-k-m}\left(\zeta\sqrt{2\gamma_{\mathrm{t}}}\right) - \sum_{n=0}^{m-1}\sum_{l=0}^{m-1} c_{n,l} \gamma_{\mathrm{t}}^{\frac{l+m+n}{2}} K_{l-m+n}\left(\zeta\sqrt{2\gamma_{\mathrm{t}}}\right) \right. \\ & \left.\left.\left.\left. + \sum_{k=0}^{m-1}\sum_{n=0}^{m-1}\sum_{l=0}^{m-1} d_{k,n,l} \gamma_{\mathrm{t}}^{\frac{k+n+l+m}{2}} K_{n+l-k-m}\left(2\zeta\sqrt{\gamma_{\mathrm{t}}}\right) \right] \right) \right) \left(1 - \frac{\Gamma(m, \frac{m}{\hat{\gamma}_{\mathrm{R}}}\gamma_{\mathrm{t}})}{\Gamma(m)} \right) \right]. \end{aligned} \tag{36}$$

and

$$\mathcal{J}_3 = \frac{1}{2\pi\zeta^{2m+n+k}} \times G_{4,2}^{1,4}\left(\frac{1}{\zeta^2} \;\middle|\; \begin{matrix}(1-(m+n),1-(m+k),1,1)\\(1,0)\end{matrix} \right). \tag{34}$$

Now, by inserting (32), (33), and (34) into (28), the proof is completed. □

B. Outage Probability

The outage probability is defined as the probability that the received SNR is less than a certain threshold γ_{t}. This metric is a well-established proxy for error performance measures in uncoded communication systems, in a modulation-agnostic fashion, i.e., not dependent on the specific modulation scheme. In fact, symbol error probability and outage probabilities often have similar trends, up to a constant scaling factor in the asymptotic regime [52]. Thus, we define the outage probability for the given dual-hop relay network as follows

$$P_{\mathrm{o}} = \Pr\left(\min(\gamma_{\mathrm{R}}, \gamma_{\mathrm{D}}) \leq \gamma_{\mathrm{t}}\right). \tag{35}$$

Theorem 6. *The outage probability for the considered dual-hop SWIPT relay network over dependent Nakagami-m fading channels is given by* (36)*.*

Proof. The outage probability given in (35) can be expressed in terms of the survival copula as follows

$$P_{\mathrm{o}} = 1 - \Pr\left(\gamma_{\mathrm{R}} > \gamma_{\mathrm{t}}, \gamma_{\mathrm{D}} > \gamma_{\mathrm{t}}\right) \tag{37}$$

$$= 1 - \hat{\mathcal{C}}\left(\overline{F}_{\gamma_{\mathrm{R}}}(\gamma_{\mathrm{t}}), \overline{F}_{\gamma_{\mathrm{D}}}(\gamma_{\mathrm{t}})\right), \tag{38}$$

where $\overline{F}_{\gamma_{\mathrm{R}}}(\gamma_{\mathrm{t}}) = 1 - F_{\gamma_{\mathrm{R}}}(\gamma_{\mathrm{t}})$ and $\overline{F}_{\gamma_{\mathrm{D}}}(\gamma_{\mathrm{t}}) = 1 - F_{\gamma_{\mathrm{D}}}(\gamma_{\mathrm{t}})$ are the survival functions of γ_{R} and γ_{D}, respectively. Now, using the fact that the FGM survival copula is same as the FGM copula, i.e., $\hat{C}_{\mathcal{F}}(u_1, u_2) = C_{\mathcal{F}}(u_1, u_2)$, inserting (14) and (17) into (38), and doing some simplifications, the proof is completed. □

C. Asymptotic Analysis

Although the analytical expressions provided in (23), (26), and (36) fully capture the system performance in terms of the ergodic capacity and the outage probability, we are interested in examining the asymptotic behavior of these metrics in the high SNR regime which can provide deeper insights into the system performance. For this purpose, we allow $\hat{\gamma}_{\mathrm{R}}$ to approach infinity; this can be justified when the relay is closer to the source, which is often the case for energy-constrained devices harvesting power from an external source.

In the following theorem, we derive the asymptotic expression of the ergodic capacity for the considered model.

Theorem 7. *In the high SNR regime, the asymptotic ergodic capacity of the SR link for the considered system model under Nakagami-m fading channel is given by*

$$\overline{\mathcal{C}}_{\mathrm{SR}}^{\infty} = \frac{1}{2\Gamma(m)\ln 2}\left(-\ln\left(\frac{m}{\hat{\gamma}_{\mathrm{R}}} + \psi(m) \right) \right), \tag{39}$$

where $\psi(.)$ is the digamma function.

Proof. Assuming the high SNR regime (i.e., $\gamma_{\rm R} \gg 1$), (24) can be written as

$$\overline{\mathcal{C}}_{\rm SR}^{\infty} = \frac{1}{2\ln 2}\int_0^{\infty} \ln\left(\gamma_{\rm R}\right) f_{\gamma_{\rm R}}(\gamma_{\rm R}) d\gamma_{\rm R} \tag{40}$$

$$\overset{(a)}{=} \frac{m^m}{2\hat{\gamma}_{\rm R}^m \ln 2}\int_0^{\infty} \gamma_{\rm R}^{m-1} \mathrm{e}^{-\frac{m}{\hat{\gamma}_{\rm R}}} \ln\left(\gamma_{\rm R}\right) d\gamma_{\rm R}, \tag{41}$$

where (a) is achieved by inserting (16) into (40). By solving the integral in (41) with the help of integral format provided in [53], the proof is completed. □

Remark 1. *An asymptotic expression for $\mathcal{C} = \min(\mathcal{C}_{\rm SR}, \mathcal{C}_{\rm RD})$ that works well under the* $\min()$ *operator in* (20) *is only valid if both average SNRs are sufficiently large, so that asymptotic high-SNR analysis is valid on both sides. For a practical perspective, it seems reasonable to consider that the SR link has a sufficiently large SNR, so that the energy harvesting and information transfer processes at the relay are successful for a proper operation. In such a case, the approximate expression in* (39) *for the ergodic capacity in the SR link is highly accurate (the asymptotic expression is tight for the SR link), and the overall capacity will be determined by the RD link as the destination node is located further away. In this regime, the asymptotic expression for the SR capacity can be safely evaluated by* (39)*, but the overall capacity is dominated by that of the RD link.*

The asymptotic outage probability for the proposed model is given by the following theorem.

Theorem 8. *In the high SNR regime, the asymptotic outage probability for the considered dual-hop SWIPT relay network over dependent Nakagami-m fading channels is given by* (42)

$$P_{\rm o}^{\infty} \approx 1 - \overline{F}_{\gamma_{\rm R}}^{\infty}(\gamma_{\rm t})\overline{F}_{\gamma_{\rm D}}(\gamma_{\rm t})\big(1 + \theta F_{\gamma_{\rm R}}^{\infty}(\gamma_{\rm t})F_{\gamma_{\rm D}}(\gamma_{\rm t})\big), \tag{42}$$

where

$$F_{\gamma_{\rm R}}^{\infty}(\gamma_{\rm R}) \approx \frac{m^m \gamma_{\rm R}^m}{\hat{\gamma}_{\rm R}^m \Gamma(m+1)}, \tag{43}$$

and $\overline{F}_{\gamma_{\rm R}}^{\infty}(\gamma_{\rm R}) = 1 - F_{\gamma_{\rm R}}^{\infty}(\gamma_{\rm R})$.

Proof. The CDF of $\gamma_{\rm R}$ at the high SNR regime can be approximated by (43) as in [52]. Now, by exploiting the FGM copula definition from (13), the outage probability in (38) can be re-written as

$$P_{\rm o} = 1 - \overline{F}_{\gamma_{\rm R}}(\gamma_{\rm t})\overline{F}_{\gamma_{\rm D}}(\gamma_{\rm t})\big(1 + \theta F_{\gamma_{\rm R}}(\gamma_{\rm t})F_{\gamma_{\rm D}}(\gamma_{\rm t})\big). \tag{44}$$

Then, by inserting the CDF of $\gamma_{\rm R}$ from (14) and the approximate CDF of $\gamma_{\rm D}$ from (43) into (44), the asymptotic outage probability can be obtained as (42) and the proof is completed. □

Remark 2. *In view of* (39)*, similar to the exact ergodic capacity derived for the SR link in* (23)*, we can see that the correlation does not affect the ergodic capacity of the SR link at the high SNR regime for a fixed transmit power. However, regarding the impact of correlation on the ergodic capacity of the RD link in* (26) *and the ergodic capacity definition in* (26)*, a positive (negative) dependence increases (decreases) the ergodic capacity of the proposed system model in the high SNR regime, by virtue of Corollary 2.*

Remark 3. *Given* (42)*, similar to the exact outage probability obtained in* (36)*, we state that the positive (negative) dependence provides a lower (higher) outage probability in the high SNR regime with a fixed transmit power. In addition, the asymptotic outage probability in* (42) *highly depends on the fading parameter m.*

V. NUMERICAL RESULTS

In this section, we evaluate the theoretical expressions previously derived, which are double-checked in all instances with Monte-Carlo (MC) simulations[2].

Fig. 2 illustrates the performance of ergodic capacity under correlated Nakagami-m fading based on the variation of PSR factor ρ for selected values of fading parameter m and dependence parameter θ. In both independent and correlated fading conditions, we can see that the capacity performance is improved as ρ increases from 0 to an optimal value and it is weakened as ρ grows from the optimal value to 1. The reason for this behavior is that as ρ increases from 0 to its optimal value, more power is allocated to the EH process, and thus, the relay node R can transmit information with a higher power, which improves the capacity performance. However, as ρ grows from its optimal amount to 1, more power is dedicated to the EH process and less power remains for SR information processing, so, the capacity value decreases. Furthermore, it can be seen that correlated fading provides better performance as compared with negative dependence structure as well as the independent case in terms of the ergodic capacity. We can also observe that as the fading severity reduces (i.e., m increases), the ergodic capacity performance ameliorates but the fading correlation effects are gradually eliminated.

The behavior of the ergodic capacity in terms of the source power $P_{\rm S}$ for the selected values of the fading and dependence parameters is shown in Fig. 3. We can see that under fixed values of the PSR factor ρ and EH efficiency κ, the ergodic capacity performance improves as $P_{\rm S}$ and m increase, as expected. Fig. 4 represents the ergodic capacity performance with respect to the EH efficiency κ for selected values of the fading and dependence parameters. It can be observed that a larger ergodic capacity is achieved when κ tends to 1 since an increment in EH efficiency leads more energy reach to the harvester in each slot. The ergodic capacity performance based on the variations of the noise power N for given values of the fading and dependence parameters is illustrated in Fig. 5, where lower values of the ergodic capacity achieve as the noise power decreases. As expected, the ergodic capacity performance also improves as m increases under both dependent and independent structures.

Fig. 6 indicates the behavior of the ergodic capacity in terms of the SR distance $d_{\rm SR}$ under different values of the

[2]Basic simulation of copula-based dependence between RVs is natively implemented in software mathematical packages such as Matlab, and more sophisticated functionalities are available through recently developed packages [54]. Besides, such dependence can also be easily implemented using state-of-the-art methods of transformation of RVs [55].

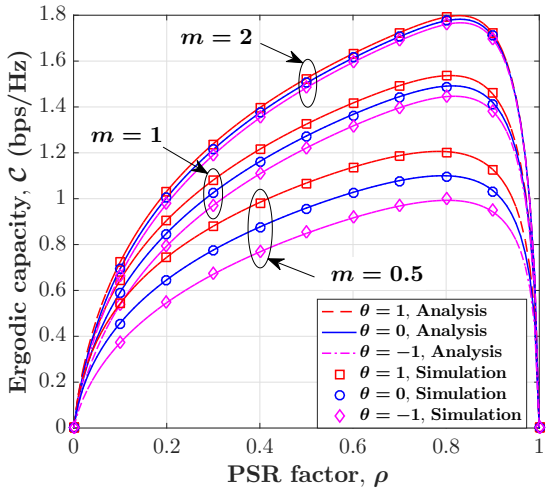

Fig. 2. Ergodic capacity versus PSR factor ρ under dependent/independent Nakagami-m fading channels when $\kappa = 0.7$, $P_{\rm S} = 10$W, $N = 10^{-2}$W, $d_{\rm SR} = d_{\rm RD} = 2$m, and $\alpha = 2.5$.

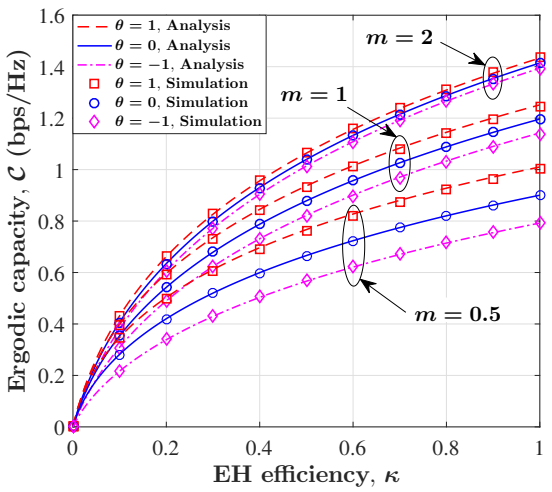

Fig. 4. Ergodic capacity versus EH efficiency κ under dependent/independent Nakagami-m fading channels when $\rho = 0.3$, $P_{\rm S} = 10$W, $N = 10^{-2}$W, $d_{\rm SR} = d_{\rm RD} = 2$m, and $\alpha = 2.5$.

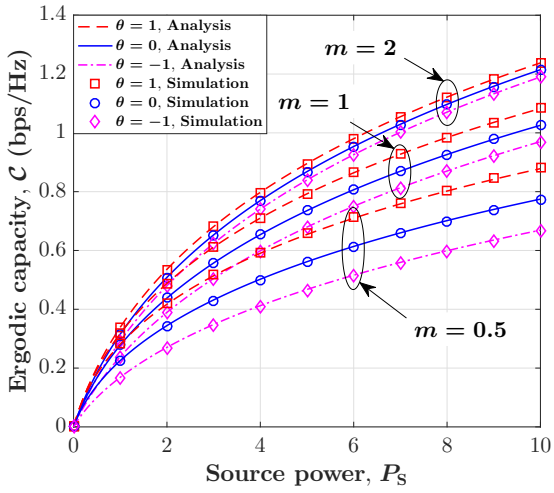

Fig. 3. Ergodic capacity versus source power $P_{\rm S}$ under dependent/independent Nakagami-m fading channels when $\kappa = 0.7$, $\rho = 0.3$, $N = 10^{-2}$W, $d_{\rm SR} = d_{\rm RD} = 2$m, and $\alpha = 2.5$.

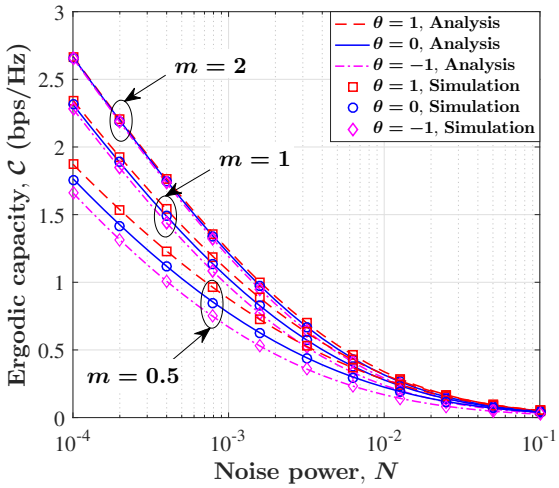

Fig. 5. Ergodic capacity versus noise power N under dependent/independent Nakagami-m fading channels when $\kappa = 0.7$, $\rho = 0.3$, $P_{\rm S} = 1$W, $d_{\rm RD} = d_{\rm SR} = 2$m, and $\alpha = 2.5$.

dependence parameter. In this case, the RD distance $d_{\rm RD}$ is set to $d_{\rm RD} = 4 - d_{\rm SR}$, and other parameters are kept fixed. For $d_{\rm SR} < 2$, it can be observed that the ergodic capacity decreases as the distance between the source node and the relay node increases. The reason is that by increasing $d_{\rm SR}$, both energy harvested and the received signal strength at the relay node decrease due to the larger path-loss $d_{\rm SR}^{\alpha}$. Therefore, the received signal strength at the destination node is poor and the ergodic capacity decreases. However, we can see that the ergodic capacity slightly increases by increasing $d_{\rm SR}$ beyond 2. This is because as the relay node gets closer to the destination ($d_{\rm RD} < 2$), even lesser values of harvested energy, the harvested energy is enough for reliable communication between the relay and the destination nodes due to smaller values of the RD path-loss $d_{\rm RD}^{\alpha}$.

Figs. 7 and 8 show the behavior of the outage probability in terms of ρ under correlated Nakagami-m fading channels for different values of the EH efficiency κ, dependence parameter θ, and source power $P_{\rm S}$. With the same argument adopted in analyzing Fig. 2, we observe that there is a trade-off between energy harvesting and information transmission in terms of the outage probability, such that the minimum outage probability is achieved for an optimal value of ρ under both correlated and independent fading scenarios. Furthermore, it is worth noting that the outage probability performance improves as the EH efficiency κ grows since the harvester gains more energy in each available slot. We can also see that the outage probability improvement is increased as $P_{\rm S}$ rises under all dependence structures. From correlation viewpoint, it can be realized from both Figs. 7 and 8 that the correlated fading provides a smaller outage probability under positive dependence structure compared with negative correlation and independent case.

This article has been accepted for publication in IEEE Transactions on Communications. This is the author's version which has not been fully edited and content may change prior to final publication. Citation information: DOI 10.1109/TCOMM.2024.3359034

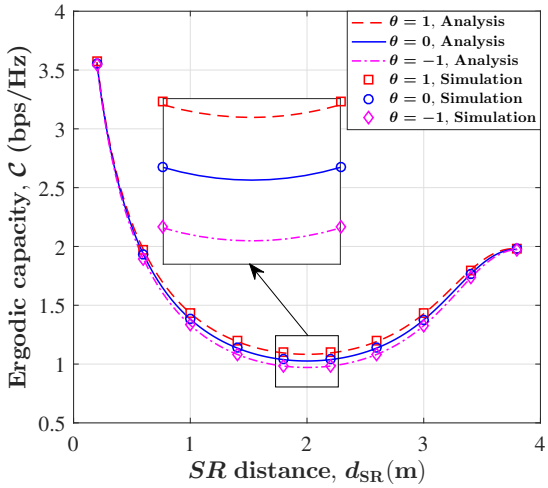

Fig. 6. Ergodic capacity versus SR distance d_{SR} under dependent/independent Nakagami-m fading channels when $\rho = 0.3$, $m = 1$, $P_{\rm S} = 10$W, $N = 10^{-2}$W, $d_{\rm RD} = 4 - d_{\rm SR}$, and $\alpha = 2.5$.

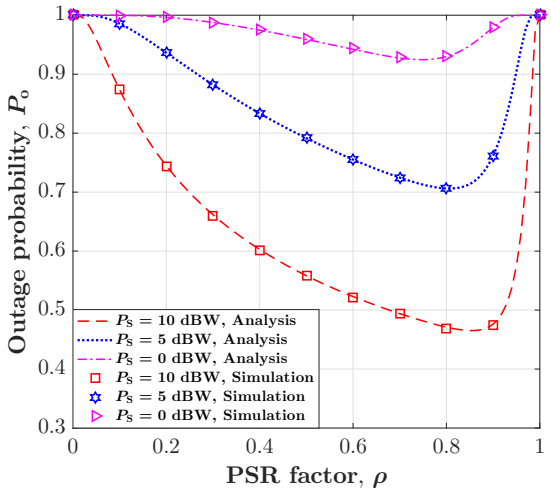

Fig. 8. Outage probability versus PSR factor ρ under dependent Nakagami-m fading channels with positive structure when $\kappa = 0.7$, $m = 1$, $\gamma_{\rm t} = 0$dB, $N = 10^{-3}$W, $d_{\rm SR} = d_{\rm RD} = 2$m, and $\alpha = 2.5$.

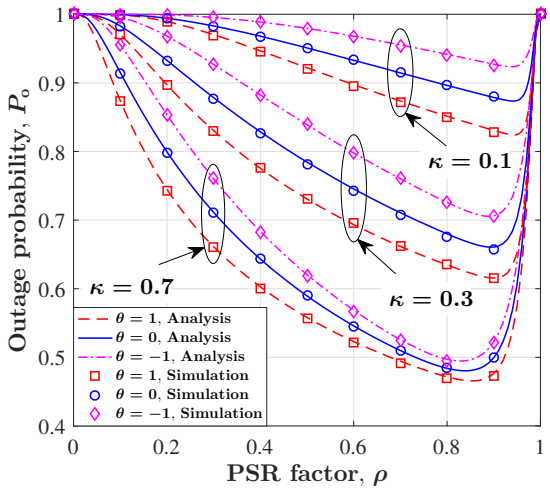

Fig. 7. Outage probability versus PSR factor ρ under dependent/independent Nakagami-m fading channels when $m = 1$, $P_{\rm S} = 10$W, $N = 10^{-3}$W, $d_{\rm SR} = d_{\rm RD} = 2$m, $\gamma_{\rm t} = 0$dB, and $\alpha = 2.5$.

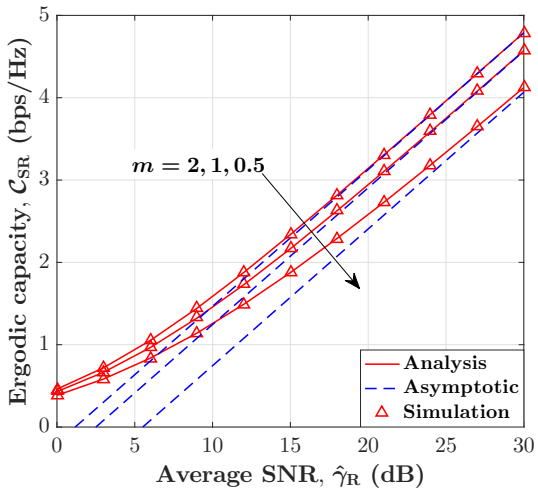

Fig. 9. Average capacity of the SR link versus $\hat{\gamma}_{\rm R}$ for different values of fading parameter m, when $P_{\rm S} = 10$W, $N = 10^{-3}$W, $d_{\rm SR} = d_{\rm RD} = 2$m, $\kappa = 0.7$, $\rho = 0.3$, and $\alpha = 2.5$.

Fig. 9 shows the exact and asymptotic behavior of the average capacity for the SR link in terms of $\hat{\gamma}_{\rm R}$. It can be seen that as $\hat{\gamma}_{\rm R}$ grows, a larger capacity is provided for the SR link. Furthermore, it becomes evident that the capacity highly depends on the fading parameter in the high SNR regime (see (39)) so that as m increases the capacity performance improves. In Fig. 10, the exact and asymptotic performance of the outage probability in terms of the average SNR $\hat{\gamma}_{\rm D}$ under positive correlation is represented. Since the approximation in (42) is based on letting $\hat{\gamma}_{\rm R} \to \infty$, it is not asymptotically tight for $\hat{\gamma}_{\rm D} \to \infty$ by construction. However, it provides an accurate lower bound to the exact OP for the entire range of SNR values. In addition, we can see that as $\hat{\gamma}_{\rm D}$ increases, the outage probability performance improves since the channel conditions become better. Furthermore, we can also observe that in both exact and asymptotic analysis, the outage probability performance highly depends on the fading parameter, namely, lower outage probability is achieved as m grows.

VI. Conclusion

In this paper, we analyzed the effect of fading correlation on the performance of SWIPT relay networks, where the power splitting relaying protocol is used for the energy harvesting process. To this end, we first provided general analytical expressions of the CDF for the product of two arbitrary dependent random variables. Then, we obtained the closed-form expressions for the ergodic capacity and outage probability under correlated Nakagami-m fading channels, using FGM copula. Our theoretical results, confirmed by simulations, show that a positive dependence between the SR and RD links has a constructive effect on the system performance, while

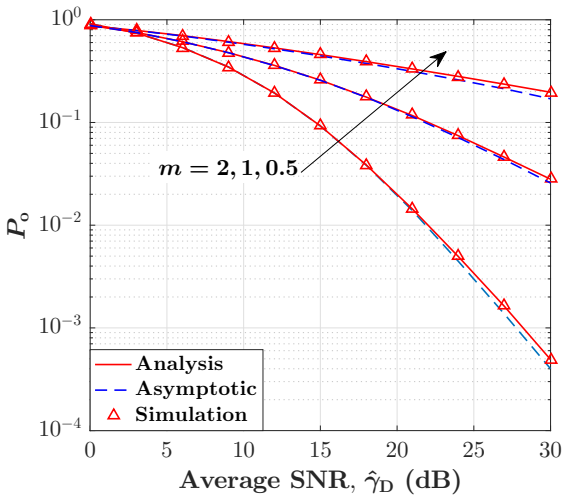

Fig. 10. Outage probability versus $\hat{\gamma}_{\rm D}$ under positive correlation for different values of fading parameter m, when $P_{\rm S} = 10$W, $N = 10^{-3}$W, $d_{\rm SR} = d_{\rm RD} = 2$m, $\kappa = 0.7$, $\rho = 0.3$, $\alpha = 2.5$, $\gamma_{\rm t} = 0$dB, and $\theta = 1$.

the converse conclusion is obtained for the case of negative dependence. These effects become more important as fading severity grows. Since copula theory can be extended to d-dimensions (i.e., beyond the two-dimensional case here considered), the scenario can be scaled to consider multiple relay networks.The derivation of additional performance metrics related to energy efficiency remain as a potential line for future research activities.

Appendix A
Proof of Theorem 2

By assuming $Y_1 = X_1 X_2$ and $Y_2 = X_1$, and exploiting the PDF of Y_1 determined in [36, Thm. 3] as:

$$f_{Y_1}(y_1) = \int_0^1 c\left(u, F_{\frac{Y_1}{Y_2}}\left(\frac{y_1}{F^{-1}_{Y_2}(u)}\right)\right) \frac{f_{\frac{Y_1}{Y_2}}\left(\frac{y_1}{F^{-1}_{Y_2}(u)}\right)}{|F^{-1}_{Y_2}(u)|} du, \tag{45}$$

the CDF of Y_1 can be defined as:

$$F_{Y_1}(t) = \int_0^1 \int_{-\infty}^{t} c\left(u, F_{\frac{Y_1}{Y_2}}\left(\frac{y_1}{F^{-1}_{Y_2}(u)}\right)\right) \frac{f_{\frac{Y_1}{Y_2}}\left(\frac{y_1}{F^{-1}_{Y_2}(u)}\right)}{|F^{-1}_{Y_2}(u)|} dy_1 du, \tag{46}$$

where $c(.)$ denotes the density of copula C. By taking change of variable $v = F_{\frac{Y_1}{Y_2}}\left(\frac{y_1}{F^{-1}_{Y_2}(u)}\right) \Rightarrow dv = \frac{f_{\frac{Y_1}{Y_2}}\left(\frac{y_1}{F^{-1}_{Y_2}(u)}\right)}{F^{-1}_{Y_2}(u)} dy_1$, and since $F^{-1}_{Y_2}(u) \geq 0 \Leftrightarrow u \geq 0$, and $F^{-1}_{Y_2}(u) \leq 0 \Leftrightarrow u \leq 0$, we have

$$\begin{aligned} F_{Y_1}(t) = &- \int_0^{F_1(0)} \int_1^{F_{\frac{Y_1}{Y_2}}\left(\frac{t}{F^{-1}_{Y_2}(u)}\right)} \frac{\partial^2}{\partial u \partial v} C(u,v) dv du \\ &+ \int_{F_1(0)}^1 \int_0^{F_{\frac{Y_1}{Y_2}}\left(\frac{t}{F^{-1}_{Y_2}(u)}\right)} \frac{\partial^2}{\partial u \partial v} C(u,v) dv du. \end{aligned} \tag{47}$$

Now, by computing the above integral, the proof is completed. The details of the proof can be obtained in [56].

Appendix B
Proof of Theorem 3

By applying the FGM copula to (9), and then first derivation with respect to $F_{G_{\rm SR}}(G_{\rm SR})$, the CDF of $\gamma_{\rm D}$ can be rewritten as:

$$\begin{aligned} F_{\gamma_{\rm D}}(\gamma_{\rm D}) = &\int_0^\infty f_{G_{\rm SR}}(g_{\rm SR}) F_{G_{\rm RD}}\left(\frac{\gamma_{\rm D}}{\hat{\gamma}_{\rm D} g_{\rm SR}}\right) \\ &\times \left[1 + \theta\left(1 - F_{G_{\rm RD}}\left(\frac{\gamma_{\rm D}}{\hat{\gamma}_{\rm D} g_{\rm SR}}\right)\right)\left(1 - 2F_{G_{\rm SR}}\left(g_{\rm SR}\right)\right)\right] dg_{\rm SR}, \end{aligned} \tag{48}$$

$$= 1 - \mathcal{I}_1 + \theta\left[-\mathcal{I}_1 + 2\mathcal{I}_2 + \mathcal{I}_3 - 2\mathcal{I}_4\right], \tag{49}$$

where

$$\mathcal{I}_1 = \int_0^\infty f_{G_{\rm SR}}(g_{\rm SR}) \overline{F}_{G_{\rm RD}}\left(\frac{\gamma_{\rm D}}{\hat{\gamma}_{\rm D} g_{\rm SR}}\right) dg_{\rm SR}, \tag{50}$$

$$\mathcal{I}_2 = \int_0^\infty f_{G_{\rm SR}}(g_{\rm SR}) \overline{F}_{G_{\rm SR}}(g_{\rm SR}) \overline{F}_{G_{\rm RD}}\left(\frac{\gamma_{\rm D}}{\hat{\gamma}_{\rm D} g_{\rm SR}}\right) dg_{\rm SR}, \tag{51}$$

$$\mathcal{I}_3 = \int_0^\infty f_{G_{\rm SR}}(g_{\rm SR}) \left(\overline{F}_{G_{\rm RD}}\left(\frac{\gamma_{\rm D}}{\hat{\gamma}_{\rm D} g_{\rm SR}}\right)\right)^2 dg_{\rm SR}, \tag{52}$$

$$\mathcal{I}_4 = \int_0^\infty f_{G_{\rm SR}}(g_{\rm SR}) \overline{F}_{G_{\rm SR}}(g_{\rm SR}) \left(\overline{F}_{G_{\rm RD}}\left(\frac{\gamma_{\rm D}}{\hat{\gamma}_{\rm D} g_{\rm SR}}\right)\right)^2 dg_{\rm SR}. \tag{53}$$

Now, by inserting the marginal CDFs and PDFs of $g_{\rm SR}$ given in (10) and (12) to above integrals and exploiting the following integral format, i.e.,

$$\int_0^\infty x^{\beta-1} \mathrm{e}^{-\left(\lambda x + \frac{\eta}{x}\right)} dx = 2\,\eta^{\frac{\beta}{2}} \lambda^{-\frac{\beta}{2}} K_{-\beta}\left(2\sqrt{\eta\lambda}\right), \tag{54}$$

the integrals $\mathcal{I}_w$ for $w \in \{1,2,3,4\}$ can be computed as:

$$\mathcal{I}_1 = \frac{m^m}{\Gamma(m)} \sum_{k=0}^{m-1} \frac{m^n \gamma_{\rm D}^n}{\hat{\gamma}_{\rm D}^n n!} \int_0^\infty g_{\rm SR}^{m-n-1} \mathrm{e}^{-m g_{\rm SR} - \frac{m\gamma_{\rm D}}{\hat{\gamma}_{\rm D} g_{\rm SR}}} dg_{\rm SR}, \tag{55}$$

$$= \frac{m^m}{\Gamma(m)} \sum_{n=0}^{m-1} \frac{2m^n}{n!} \left(\frac{\gamma_{\rm D}}{\hat{\gamma}_{\rm D}}\right)^{\frac{m+n}{2}} K_{n-m}\left(2m\sqrt{\frac{\gamma_{\rm D}}{\hat{\gamma}_{\rm D}}}\right), \tag{56}$$

$$\begin{aligned} \mathcal{I}_2 = &\frac{m^m}{\Gamma(m)} \sum_{k=0}^{m-1} \sum_{n=0}^{m-1} \frac{m^{k+n} \gamma_{\rm D}^n}{\hat{\gamma}_{\rm D}^n k! n!} \\ &\times \int_0^\infty g_{\rm SR}^{k-n+m-1} \mathrm{e}^{-2m g_{\rm SR} - \frac{m\gamma_{\rm D}}{\hat{\gamma}_{\rm D} g_{\rm SR}}} dg_{\rm SR}, \end{aligned} \tag{57}$$

$$\begin{aligned} = &\frac{m^m}{\Gamma(m)} \sum_{k=0}^{m-1} \sum_{n=0}^{m-1} \frac{2^{\frac{-k-m+n+2}{2}} m^{k+n}}{\hat{\gamma}_{\rm D}^{\frac{k+n+m}{2}} k! n!} \gamma_{\rm D}^{\frac{k+n+m}{2}} \\ &\times K_{n-k-m}\left(2m\sqrt{\frac{2\gamma_{\rm D}}{\hat{\gamma}_{\rm D}}}\right), \end{aligned} \tag{58}$$

$$\mathcal{I}_3 = \frac{m^m}{\Gamma(m)} \sum_{n=0}^{m-1} \sum_{l=0}^{m-1} \frac{1}{n!l!} \times \int_0^\infty g_{\mathrm{SR}}^{m-1} \mathrm{e}^{-mg_{\mathrm{SR}} - \frac{2m\gamma_{\mathrm{D}}}{\hat{\gamma}_{\mathrm{D}} g_{\mathrm{SR}}}} \left(\frac{m\gamma_{\mathrm{D}}}{\hat{\gamma}_{\mathrm{D}} g_{\mathrm{SR}}} \right)^{n+l} dg_{\mathrm{SR}}, \quad (59)$$

$$= \frac{m^m}{\Gamma(m)} \sum_{n=0}^{m-1} \sum_{l=0}^{m-1} \frac{2^{\frac{-l+m-n+2}{2}} m^{l+n}}{\hat{\gamma}_{\mathrm{D}}^{\frac{l+m+n}{2}} n!l!} \gamma_{\mathrm{D}}^{\frac{l+m+n}{2}} \times K_{l-m+n} \left(2m \sqrt{\frac{2\gamma_{\mathrm{D}}}{\hat{\gamma}_{\mathrm{D}}}} \right), \quad (60)$$

and

$$\mathcal{I}_4 = \frac{m^m}{\Gamma(m)} \sum_{k=0}^{m-1} \sum_{n=0}^{m-1} \sum_{l=0}^{m-1} \frac{m^{k+n+l} \gamma_{\mathrm{D}}^{n+l}}{\hat{\gamma}_{\mathrm{D}}^{n+l} k!n!l!} \times \int_0^\infty g_{\mathrm{SR}}^{k-n-l+m-1} e^{-2mg_{\mathrm{SR}} - \frac{2m\gamma_{\mathrm{D}}}{\hat{\gamma}_{\mathrm{D}} g_{\mathrm{SR}}}} dg_{\mathrm{SR}}, \quad (61)$$

$$= \frac{m^m}{\Gamma(m)} \sum_{k=0}^{m-1} \sum_{n=0}^{m-1} \sum_{l=0}^{m-1} \frac{2m^{k+n+l}}{\hat{\gamma}_{\mathrm{D}}^{\frac{k+n+l+m}{2}} k!n!l!} \gamma_{\mathrm{D}}^{\frac{k+n+l+m}{2}} \times K_{n+l-k-m} \left(4m \sqrt{\frac{\gamma_{\mathrm{D}}}{\hat{\gamma}_{\mathrm{D}}}} \right). \quad (62)$$

Finally, by plugging (56)-(62) into (49) and doing some algebraic simplifications, the proof is completed.

REFERENCES

[1] K. David and H. Berndt, "6G vision and requirements: Is there any need for beyond 5G?" *IEEE Veh. Technol. Mag.*, vol. 13, no. 3, pp. 72–80, 2018.

[2] C. Huang, R. Zhang, and S. Cui, "Throughput maximization for the Gaussian relay channel with energy harvesting constraints," *IEEE J. Sel. Areas Commun.*, vol. 31, no. 8, pp. 1469–1479, 2012.

[3] R. Jiang, K. Xiong, P. Fan, Y. Zhang, and Z. Zhong, "Optimal design of SWIPT systems with multiple heterogeneous users under non-linear energy harvesting model," *IEEE Access*, vol. 5, pp. 11 479–11 489, 2017.

[4] K. Xiong, B. Wang, and K. R. Liu, "Rate-energy region of SWIPT for MIMO broadcasting under nonlinear energy harvesting model," *IEEE Trans. Wireless Commun.*, vol. 16, no. 8, pp. 5147–5161, 2017.

[5] L. R. Varshney, "Transporting information and energy simultaneously," in *2008 IEEE International Symposium on Information Theory*, 2008, pp. 1612–1616.

[6] X. Lu, P. Wang, D. Niyato, D. I. Kim, and Z. Han, "Wireless networks with RF energy harvesting: A contemporary survey," *IEEE Commun. Surv. Tutor.*, vol. 17, no. 2, pp. 757–789, 2014.

[7] X. Zhou, R. Zhang, and C. K. Ho, "Wireless information and power transfer: Architecture design and rate-energy tradeoff," *IEEE Trans. Commun.*, vol. 61, no. 11, pp. 4754–4767, 2013.

[8] A. A. Nasir, X. Zhou, S. Durrani, and R. A. Kennedy, "Relaying protocols for wireless energy harvesting and information processing," *IEEE Trans. Wireless Commun.*, vol. 12, no. 7, pp. 3622–3636, 2013.

[9] G. Pan and C. Tang, "Outage performance on threshold AF and DF relaying schemes in simultaneous wireless information and power transfer systems," *AEU - Int. J. Electron. Commun.*, vol. 71, pp. 175–180, 2017.

[10] N. T. Do, D. B. da Costa, T. Q. Duong, V. N. Q. Bao, and B. An, "Exploiting direct links in multiuser multirelay SWIPT cooperative networks with opportunistic scheduling," *IEEE Trans. Wireless Commun.*, vol. 16, no. 8, pp. 5410–5427, 2017.

[11] X. Di, K. Xiong, P. Fan, and H.-C. Yang, "Simultaneous wireless information and power transfer in cooperative relay networks with rateless codes," *IEEE Trans. Veh. Technol.*, vol. 66, no. 4, pp. 2981–2996, 2016.

[12] K. M. Rabie, B. Adebisi, and M.-S. Alouini, "Half-duplex and full-duplex AF and DF relaying with energy-harvesting in log-normal fading," *IEEE Trans. Green Commun.*, vol. 1, no. 4, pp. 468–480, 2017.

[13] T. Li, P. Fan, and K. B. Letaief, "Outage probability of energy harvesting relay-aided cooperative networks over Rayleigh fading channel," *IEEE Trans. Veh. Technol.*, vol. 65, no. 2, pp. 972–978, 2015.

[14] H. Lee, C. Song, S.-H. Choi, and I. Lee, "Outage probability analysis and power splitter designs for SWIPT relaying systems with direct link," *IEEE Commun. Lett.*, vol. 21, no. 3, pp. 648–651, 2016.

[15] Y. Lou, Y. Zheng, J. Cheng, and H. Zhao, "Performance of SWIPT-Based Differential AF Relaying Over Nakagami-m Fading Channels With Direct Link," *IEEE Wireless Commun. Lett.*, vol. 7, no. 1, pp. 106–109, 2017.

[16] S. Zhong, H. Huang, and R. Li, "Outage probability of power splitting SWIPT two-way relay networks in Nakagami-m fading," *EURASIP J. Wirel. Commun. Netw.*, vol. 2018, no. 1, pp. 1–8, 2018.

[17] K. Rabie, B. Adebisi, G. Nauryzbayev, O. S. Badarneh, X. Li, and M.-S. Alouini, "Full-duplex energy-harvesting enabled relay networks in generalized fading channels," *IEEE Wireless Commun. Lett.*, vol. 8, no. 2, pp. 384–387, 2018.

[18] G. Nauryzbayev, K. M. Rabie, M. Abdallah, and B. Adebisi, "On the Performance Analysis of WPT-Based Dual-Hop AF Relaying Networks in α-μ Fading," *IEEE Access*, vol. 6, pp. 37 138–37 149, 2018.

[19] A. U. Makarfi, R. Kharel, K. M. Rabie, X. Li, O. S. Badarneh, G. Nauryzbayev, S. Arzykulov, and O. Kaiwartya, "Performance Analysis of SWIPT Networks over Composite Fading Channels," in *2020 IEEE Eighth International Conference on Communications and Networking (ComNet)*, 2020, pp. 1–7.

[20] S. Solanki, V. Singh, and P. K. Upadhyay, "RF Energy Harvesting in Hybrid Two-Way Relaying Systems With Hardware Impairments," *IEEE Trans. Veh. Technol.*, vol. 68, no. 12, pp. 11 792–11 805, 2019.

[21] D. Kumar, P. K. Singya, and V. Bhatia, "ASER Analysis of Hybrid Receiver Based SWIPT Two-Way Relay Network," *IEEE Trans. Veh. Technol.*, vol. 70, no. 10, pp. 10 018–10 030, 2021.

[22] D. Kumar, P. K. Singya, J. Nebhen, and V. Bhatia, "Performance of SWIPT-Enabled FD TWR Network With Hardware Impairments and Imperfect CSI," *IEEE Syst. J.*, vol. 17, no. 1, pp. 1224–1234, 2023.

[23] L. Fan, R. Zhao, F.-K. Gong, N. Yang, and G. K. Karagiannidis, "Secure multiple amplify-and-forward relaying over correlated fading channels," *IEEE Trans. Commun.*, vol. 65, no. 7, pp. 2811–2820, 2017.

[24] L. Fan, X. Lei, N. Yang, T. Q. Duong, and G. K. Karagiannidis, "Secrecy cooperative networks with outdated relay selection over correlated fading channels," *IEEE Trans. Veh. Technol.*, vol. 66, no. 8, pp. 7599–7603, 2017.

[25] Y. Li, Q. He, and R. S. Blum, "On the product of two correlated complex Gaussian random variables," *IEEE Signal Process. Lett.*, vol. 27, pp. 16–20, 2019.

[26] N. Bhargav, C. R. N. da Silva, Y. J. Chun, É. J. Leonardo, S. L. Cotton, and M. D. Yacoub, "On the Product of Two κ-μ Random Variables and its Application to Double and Composite Fading Channels," *IEEE Trans. Wireless Commun.*, vol. 17, no. 4, pp. 2457–2470, 2018.

[27] S. Nadarajah and T. K. Pogány, "On the distribution of the product of correlated normal random variables," *Comptes Rendus. Mathématique*, vol. 354, no. 2, pp. 201–204, 2016.

[28] S. Livieratos, A. Voulkidis, G. Chatzarakis, and P. Cottis, "Correlated phenomena in wireless communications: A copula approach," in *Applications of Mathematics and Informatics in Science and Engineering*. Springer, 2014, pp. 95–104.

[29] M. H. Gholizadeh, H. Amindavar, and J. A. Ritcey, "On the capacity of MIMO correlated Nakagami-m fading channels using copula," *EURASIP J. Wirel. Commun. Netw.*, vol. 2015, no. 1, pp. 1–11, 2015.

[30] F. R. Ghadi and G. A. Hodtani, "Copula function-based analysis of outage probability and coverage region for wireless multiple access communications with correlated fading channels," *IET Communun.*, vol. 14, no. 11, pp. 1805–1811, 2020.

[31] ——, "Copula-based analysis of physical layer security performances over correlated Rayleigh fading channels," *IEEE Trans. Inf. Forensics Secur.*, vol. 16, pp. 431–440, 2020.

[32] E. A. Jorswieck and K.-L. Besser, "Copula-based bounds for multi-user communications–Part I: Average Performance," *IEEE Commun. Lett.*, vol. 25, no. 1, pp. 3–7, 2020.

[33] K.-L. Besser and E. A. Jorswieck, "Copula-based bounds for multi-user communications–Part II: Outage Performance," *IEEE Commun. Lett.*, vol. 25, no. 1, pp. 8–12, 2020.

[34] F. R. Ghadi, G. A. Hodtani, and F. J. López-Martínez, "The role of correlation in the doubly dirty fading MAC with side information at the transmitters," *IEEE Wireless Commun. Lett.*, vol. 10, no. 9, pp. 2070–2074, 2021.

[35] K.-L. Besser and E. A. Jorswieck, "Bounds on the secrecy outage probability for dependent fading channels," *IEEE Trans. Commun.*, vol. 69, no. 1, pp. 443–456, 2020.

[36] F. R. Ghadi, F. J. Martin-Vega, and F. J. López-Martínez, "Capacity of backscatter communication under arbitrary fading dependence," *IEEE Trans. Veh. Technol.*, 2022.

[37] F. R. Ghadi and W.-P. Zhu, "Performance Analysis over Correlated/Independent Fisher-Snedecor $\mathcal{F}$ Fading Multiple Access Channels," *IEEE Trans. Veh. Technol.*, 2022.

[38] A. Tarrías-Muñoz, J. L. Matez-Bandera, P. Ramírez-Espinosa, and F. J. López-Martínez, "Effect of correlation between information and energy links in secure wireless powered communications," *IEEE Trans. Inf. Forensics Secur.*, vol. 16, pp. 3780–3789, 2021.

[39] S. Fernández, F. J. López-Martínez, F. H. Gregorio, and J. E. Cousseau, "Secure full-duplex wireless power transfer systems with energy-information correlation," *IEEE Access*, vol. 10, pp. 16 952–16 968, 2022.

[40] J. D. Griffin and G. D. Durgin, "Link envelope correlation in the backscatter channel," *IEEE Commun. Lett.*, vol. 11, no. 9, pp. 735–737, 2007.

[41] Y. Zhang, F. Gao, L. Fan, X. Lei, and G. K. Karagiannidis, "Backscatter Communications Over Correlated Nakagami- m Fading Channels," *IEEE Trans. Commun.*, vol. 67, no. 2, pp. 1693–1704, 2019.

[42] D. Deng, M. Yu, J. Xia, Z. Na, J. Zhao, and Q. Yang, "Wireless powered cooperative communications with direct links over correlated channels," *Phys. Commun.*, vol. 28, pp. 147–153, 2018. [Online]. Available: https://www.sciencedirect.com/science/article/pii/S187449071830051X

[43] L. Mohjazi, S. Muhaidat, M. Dianati, and M. Al-Qutayri, "Performance analysis of SWIPT relay networks with noncoherent modulation," *IEEE Trans. Green Commun.*, vol. 2, no. 4, pp. 1072–1086, 2018.

[44] Y. Zhang and B. Clerckx, "Waveform design for wireless power transfer with power amplifier and energy harvester non-linearities," *IEEE Trans. Signal Process.*, vol. 71, pp. 2638–2653, 2023.

[45] Y. Chen, R. Shi, and M. Long, "Performance analysis of amplify-and-forward relaying with correlated links," *IEEE Trans. Veh. Technol.*, vol. 62, no. 5, pp. 2344–2349, 2013.

[46] S. R, M. D. Selvaraj, and R. Roy, "On the error and outage performance of decode-and-forward cooperative selection diversity system with correlated links," *IEEE Trans. Veh. Technol.*, vol. 64, no. 8, pp. 3578–3593, 2015.

[47] R. B. Nelsen, *An introduction to copulas*. Springer Science & Business Media, 2007.

[48] S. Sriboonchitta and V. Kreinovich, "Why are FGM copulas successful? A simple explanation," *Advances in Fuzzy Systems*, vol. 2018, 2018.

[49] J. N. Laneman, D. N. Tse, and G. W. Wornell, "Cooperative diversity in wireless networks: Efficient protocols and outage behavior," *IEEE Trans Inf. Theory*, vol. 50, no. 12, pp. 3062–3080, 2004.

[50] V. Adamchik and O. Marichev, "The algorithm for calculating integrals of hypergeometric type functions and its realization in REDUCE system," in *Proceedings of the international symposium on Symbolic and algebraic computation*, 1990, pp. 212–224.

[51] A. Prudnikov, Y. A. Brychkov, and O. Marichev, "More Special Functions (Integrals and Series vol 3)," 1990.

[52] Z. Wang and G. Giannakis, "A simple and general parameterization quantifying performance in fading channels," *IEEE Trans. Commun.*, vol. 51, no. 8, pp. 1389–1398, 2003.

[53] https://www.wolframcloud.com/obj/frostamigh/Published/Integral.Asymptotic.nb.

[54] M. Coblenz, "MATVines: A vine copula package for MATLAB," *SoftwareX*, vol. 14, p. 100700, 2021. [Online]. Available: https://www.sciencedirect.com/science/article/pii/S2352711021000455

[55] H. Joe, *Dependence modeling with copulas*. CRC press, 2014.

[56] S. Ly, K.-H. Pho, S. Ly, and W.-K. Wong, "Determining distribution for the product of random variables by using copulas," *Risks*, vol. 7, no. 1, p. 23, 2019.